3D High Content Imaging of Optically-Cleared Microtissues for Screening Antiproliferative Cancer Drugs

Thomas S. Villani, Graeme Gardner, Michael Johnson, Nick Crider
Visikol Inc, 675 US Highway 1, North Brunswick, NJ, 08902

Highlights

When combined with high content confocal microscopy, Visikol® HISTO-M™ allows the interior environment of 3D cell cultures to be imaged, dramatically improving the number of cells detected in microtissues.

- > 3-fold increase in detectable cells within 3D cell cultures.
- Designed for high-throughput applications and automation.

Introduction

The use of *in vitro* three-dimensional (3D) cell cultures has increased dramatically for drug discovery since 3D cell culture models more accurately mimic the *in vivo* environment compared to traditional monolayer cultures[1]. However, current imaging-based analysis of these 3D cultures relies upon techniques developed originally for 2D cell culture. Due to the thickness of 3D cell cultures, typically >100 µm, light scattering does not permit imaging of the center of the microtissue[2]. This technical limitation introduces a sampling bias in imaging analysis, since only the exterior cells can be imaged. This problem should be solved to obtain the most useful and accurate survey of the cellular environment and response of the microtissue.

It was sought to solve the problem of microtissue opacity by employing an optical clearing agent designed specifically for microtissues, Visikol HISTO-M. Here, we combine 3D InSight™ NCI-H2170 Tumor Microtissues and Visikol HISTO-M clearing agent to illustrate the power of tissue clearing on high content screening of antiproliferative cancer drugs.

Materials and Methods

Reagents and cell culture

NCI-H2170 lung cancer microtissues were obtained from InSphero Inc. Antibodies and fluorescent dyes were obtained from Invitrogen. Cisplatin was obtained from Sigma Aldrich.

Treatment of microtissues with antiproliferative cisplatin

Microtissues were treated with antiproliferative compound (cisplatin) on day 0, and again on days 3 and 6. Cisplatin was dissolved in DMSO, and from this stock solution, 10-fold serial dilutions were prepared to make 100x working dilutions. Compound was diluted to final assay concentration in growth media. The assayed range of concentrations was 1 mM, 10 µM, 1 µM, 100 nM, and vehicle control.

Fixation and immunolabeling

On day 8, microtissues were fixed using 10% NBF, followed by washing in PBS to remove fixative. Microtissues were treated with methanol, followed by 20% DMSO/methanol to improve penetration of antibodies and stains. Microtissues were blocked with 10% donkey serum, then incubated with rabbit anti-Ki67 antibody (1:250 dilution, AbCam Cat# 15580) with goat anti-rabbit AlexaFluor594 conjugated secondary (1:250 dilution, ThermoFisher Cat#: R37117) to label proliferating cells. Nuclei counterstained with SYTOX green (ThermoFisher).

Clearing and high throughput imaging of microtissues

Microtissues were dehydrated with methanol, then cleared with Visikol HISTO-M. Imaging of microtissue plates was accomplished with Corning Ultra-Low Attachment Round-bottom plates and the CX7 (ThermoFisher) High Content Confocal Imager. Z-stacks were collected for each tissue, using 10 µm steps. Images were processed using automated ImageJ macros, and cells were counted using CellProfiler.

Results and Discussion

Visikol HISTO-M enables visualization of microtissue interior

As seen in Figure 1A, when imaging non-cleared microtissues, the interior of the microtissue appears dark, as light scattering drastically reduces signal due to the opacity of the microtissues, causing the "eclipsing" effect. Using Visikol HISTO-M, light scattering was greatly reduced, allowing for comprehensive profiling of the interior of the microtissues, shown in Figure 1B. Note that Z-projections of non-cleared microtissues obscures "eclipsing" that occurs from microtissue opacity, which can result in misleading data.

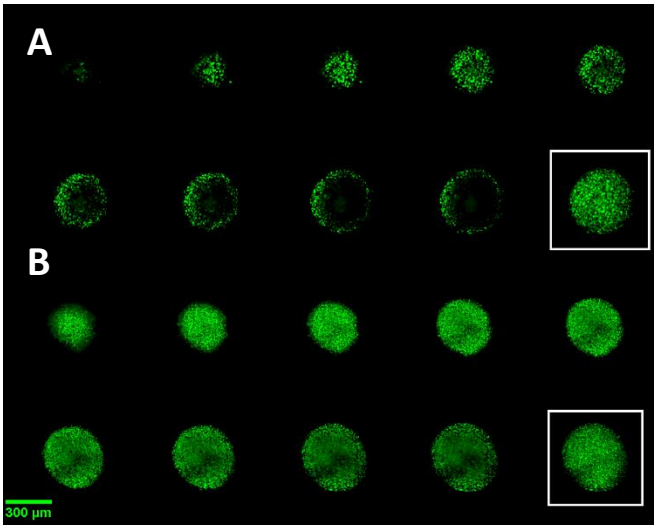

Figure 1. Montage of slices from confocal image z-stack, nuclei stained with SYTOX green; A) Non-cleared microtissue; B) Cleared microtissue; Z-projections are outlined in white; z-projections mask difficulty of imaging non-cleared microtissues since z-projections hide the eclipsing that occurs in imaging. Cleared microtissues show no eclipsing, interior cells are visible.

Visikol HISTO-M increases detectable cells in interior

CellProfiler was used for automated cell-counting of the confocal image stacks. The detected cell outlines, shown in Figure 2A, show that as the image stack progresses into the non-cleared microtissue, fewer and fewer cells are detected in the center of each plane, until only the periphery is detectable. This is due to light scattering caused by the opacity of non-cleared microtissues, which limits imaging to approximately 20-50 µm depth, even with confocal microscopy. With cleared microtissues, as shown in Figure 2B, cells are detectable across the entire image plane, deep into the microtissue. Cell counts for Figures 2A and 2B are quantified in Figure 2C. On average, 3-fold more cells were detected on each plane of the cleared microtissue than the non-cleared microtissue. The effect was even more dramatic deeper in the microtissue; at 120 µm depth, 7-fold more cells were detectable.

When conducting confocal imaging of microtissues without clearing, only the outermost cells are detected due to light scattering that reduces signal to noise. Use of a tissue clearing agent greatly increases the number of cells detectable by high content imaging. The non-adherent surface coating of InSphero assay plates was chemically compatible with Visikol HISTO-M. The clearing process takes only minutes, and is done within the well plate.

Case study: Antiproliferative assay on NCI-H2170 microtissues

Cisplatin treated and control microtissues were imaged using a CX7 High Content Imager (ThermoFisher) to obtain multicolor image stacks with a 10 um z-step size. Ki67 was used as a marker for proliferation. Cells were counted automatically with CellProfiler, giving total cell counts and Ki67+ cell counts. Ki67%, the ratio of Ki67+ to total cells, was used as the measurement of proliferation to construct dose response curves. Dose response curves were constructed for cleared and non-cleared microtissues, shown in Figure 3.

As can be easily discerned from the dose response curves shown in Figure 3A, there was a significant and measurable difference between dose response curves calculated from cleared and non-cleared microtissues. Visikol HISTO-M cleared samples show increased sensitivity to detect inhibitory activity (detected at 1 uM, compared to 10 uM required to detect signal for uncleared control samples). Furthermore, the IC_{50} value measured for Visikol HISTO-M (5.38 uM) is approximately 2x lower than calculated with uncleared control samples (10.8 uM). These results were comparable with reported IC_{50} values. Visikol HISTO-M increases sensitivity to detect inhibition due to the increased number of cells surveyed compared to the non-cleared controls.

Another advantage of Visikol HISTO-M cleared microtissues is demonstrated by measuring the absolute reduction of proliferation score in cleared and un-cleared microtissues. As can be seen in Figure 3B, the cell proliferation score reduction for uncleared tissues measures a greater reduction than for cleared tissues, which suggests that the non-cleared tissues give a falsely high rate of proliferation reduction. This is due to the bias toward surface-layer cells in imaging un-cleared tissues, which are more likely to be proliferating and likewise affected by cisplatin, and so shows a falsely overestimated response. It is important to note that this dramatic bias is

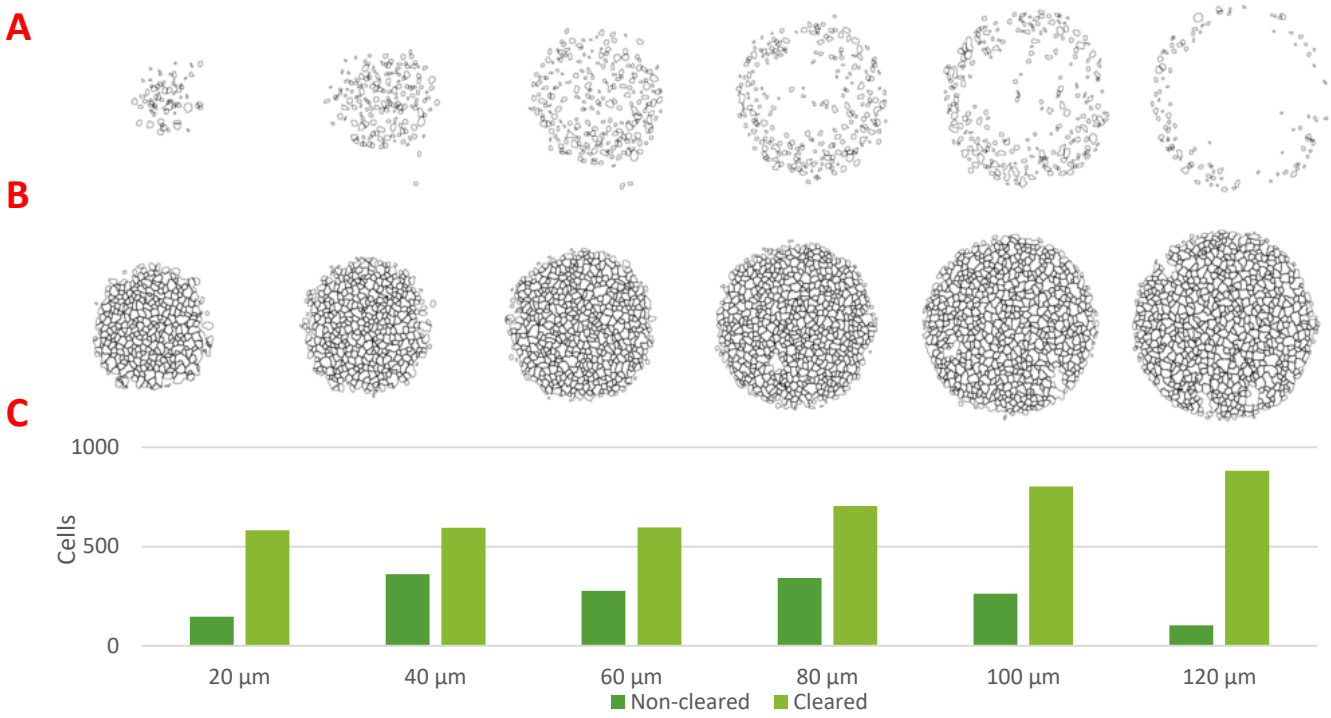

Figure 2. Outlines of cells detected by CellProfiler in InSphero NCI-H2170 lung cancer microtissues treated with 100 nM cisplatin. 20 µm optical-sections (20-120 um) shown left to right for A) Non-cleared microtissues and B) Microtissues cleared with Visikol HISTO-M; C) Cell counts for each z-plane in cleared and non-cleared microtissues from A) and B). Far more cells can be detected at each z-plane in cleared microtissues.

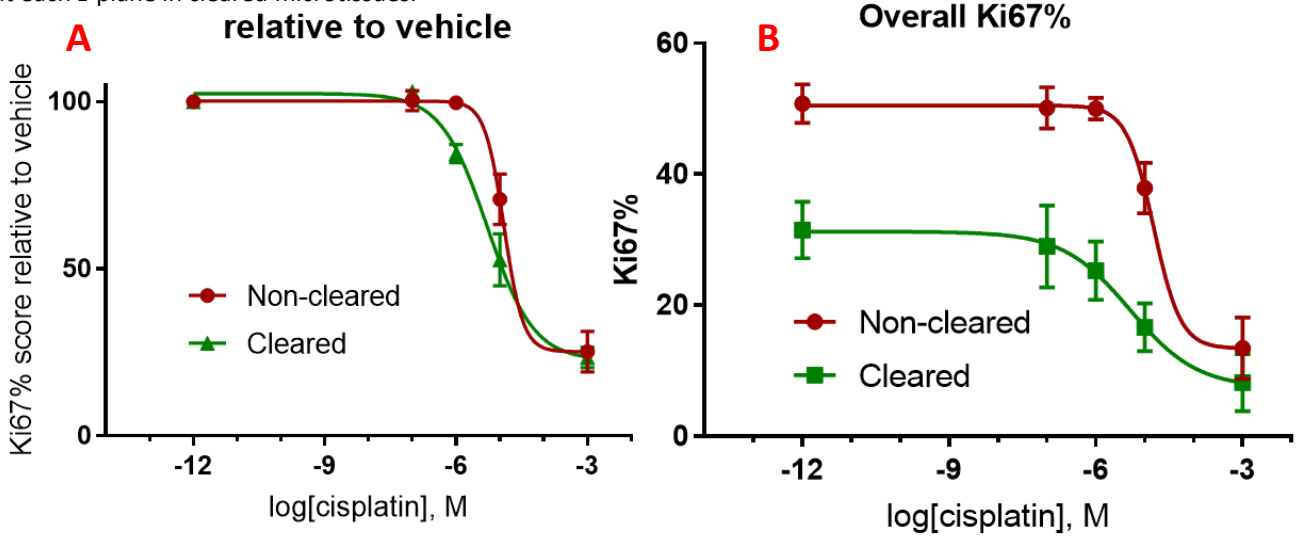

Figure 3. Antiproliferation dose response curves for cisplatin-treated NCI-H2170 microtissues A) relative to vehicle control cell proliferation score; B) showing absolute Ki67% proliferation score.

detectable even when the NCI-H2170/NHDF microtissue used consists of proliferating tumor cells forming a layer upon a fibroblast core, which is mostly non-proliferative due to cell type and oxygen/nutrient depletion. This reinforces the importance of interior tissue clearance when using models where tumor cells integrate with fibroblasts in a more evenly disbursed fashion throughout the microtissue.

Spatial Dose Response

The data from the cleared microtissues can be further processed to generate dose response as a function of distance from the center of the microtissue, split into inner, middle, and outer thirds, as shown in Figure 4. With spatial dose response data, the ability of a compound to penetrate to the center and

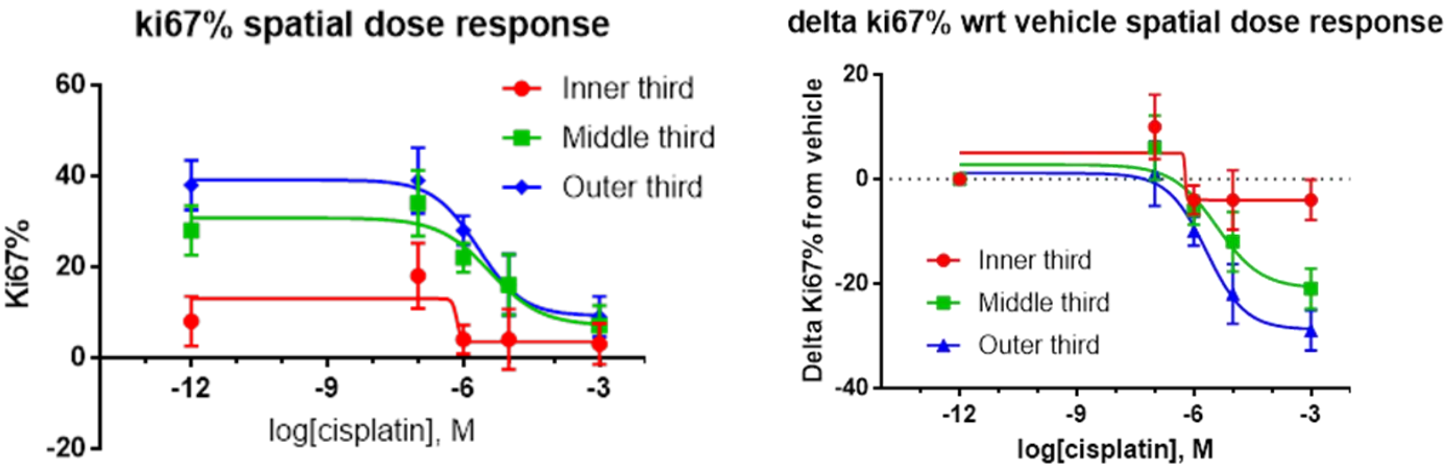

Figure 4. Antiproliferation spatial dose response curves constructed from data obtained from cleared NCI-H2170 microtissues by splitting cells into innermost third, middle third, and outer third of cells to examine difference in response.

Other 3D Imaging Endpoints

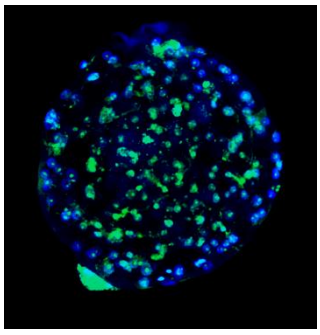

Cell viability (Calcein AM)

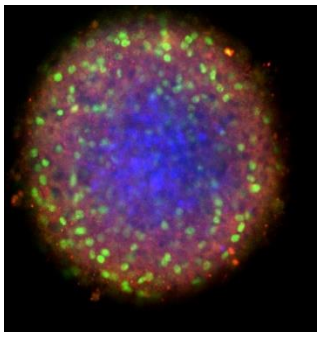

Apoptosis (Caspase-3)

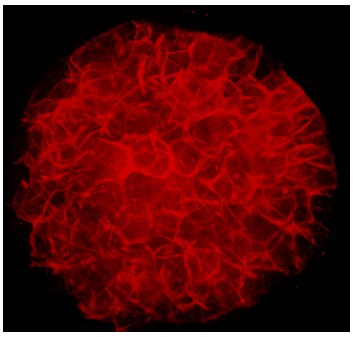

Cell adhesion (E-cadherin)

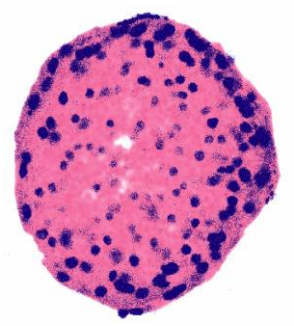

Fluorescent "H&E"

effect the deeper layers of cells can be assessed. As can be seen, proliferation of the innermost cells is significantly different than middle and outer cell layers. As expected, there was a substantial difference in antiproliferative activity of cisplatin is observed in the middle and outer cells compared to the inner cells. In this type of co-culture tumor microtissue, fibroblasts typically migrate to the center of the microtissue during self-assembly; this cellular organization may explain why little proliferation is observed in the center of the microtissue.

References

1. LaBarbera, D. V., Reid, B. G., & Yoo, B. H. (2012). The multicellular tumor spheroid model for high-throughput cancer drug discovery. *Expert opinion on drug discovery*, *7*(9), 819-830.
2. Kabadi, P. K., Vantangoli, M. M., Rodd, A. L., Leary, E., Madnick, S. J., Morgan, J. R., & Boekelheide, K. (2015). Into the depths: Techniques for in vitro three-dimensional microtissue visualization. *Biotechniques*, *59*(5), 279.
3. Quisque Yang, W., Soares, J., Greninger, P., Edelman, E. J., Lightfoot, H., Forbes, S., & Ramaswamy, S. (2012). Genomics of Drug Sensitivity in Cancer (GDSC): a resource for therapeutic biomarker discovery in cancer cells. *Nucleic acids research*, *41*(D1), D955-D961.

Conclusions

- Visikol HISTO-M is compatible with immunolabeling and fluorescent staining of microtissues.
- Clearing microtissues with Visikol HISTO-M enables visualization of the interior of microtissues.
- Cleared microtissues deliver >3x higher cell counts with high-content confocal imaging assays.
- Data obtained from Visikol HISTO-M better represents the microtissue since interior cells are detectable.

Getting Started

1. Visit www.visikol.com to learn more about using Visikol HISTO-M with microtissues.
2. Consult with our scientists to develop a customized labeling and imaging workflow.
3. Collaborations begin with pilot projects which can then be scaled up according to your requirements.
4. We work end-to-end to help you take advantage of 3D High Content Imaging assays in your workflow.